Special Feature: Power Electronics for Hybrid Vehicles

Research Report

Electromagnetic Torque Converter for Hybrid Electric Vehicles

Takao Watanabe, Shu Asami, Eiji Tsuchiya, Masaki Ebina, Yasumitsu Osada, Tomoyuki Toyama and Akira Murakami

Report received on May 19, 2017

ABSTRACT This paper presents a new electro-magnetic torque converter (eMAT) that we developed as a drivetrain component to improve fuel economy and downsize the drivetrain system of hybrid electric vehicles (HEVs). The eMAT is composed of a set of double rotors and a stator. The eMAT works as a high-efficiency torque converter and as a traction motor with an automatic transmission for HEVs. Moreover, it has new features that are not found in normal electric motors, thereby providing benefits for a new powertrain system. First, the structure of the eMAT is introduced and its unique features are explained. Second, a prototype eMAT is described, which has a compact structure that allows it to be mounted on a vehicle, and its experimentally measured transmission efficiency is discussed. Finally, we focus on one of the eMAT's unique features: the ability to suppress vibration torque. In order to leverage the eMAT features for use in a drivetrain component, a control design concept is then presented.

KEYWORDS Hybrid Electric Vehicle, Fuel Economy, Electro-magnetic Torque Converter, Vibrating Torque Suppression

1. Introduction

With growing concerns about global warming, depletion of fossil fuels, and air pollution, the importance of eco-friendly vehicles with low CO_2 emissions and exhaust free of environmental pollutants is increasing. A hybrid electric vehicle (HEV) is one of the most practical options for realizing eco-friendly vehicles. In order to satisfy the demands of automotive consumers and eventually to increase the number of HEVs, further improvement in the fuel economy of HEVs is required. Hence, improvement of the efficiency of hybrid powertrain systems is still a major area of development.

Hybrid powertrains improve fuel economy by electric motor driving during low-load driving conditions and vehicle energy recuperation using the electric motor during braking conditions. In addition to these factors, an improvement in transmission efficiency would also improve the fuel economy. To achieve this, power losses in the transmission system need to be reduced. Depending on the hybrid powertrain configuration, the total loss as well as its generation mechanism differ. Hence, it is important to investigate the optimal configuration considering a new drivetrain component that improves the system efficiency of the hybrid powertrain.

In this paper, we present a new electric machine to improve hybrid powertrain efficiency and describe its use in a new hybrid powertrain system configuration. The electric machine is composed of a set of double rotors and a stator, and is called an electro-magnetic torque converter—hereafter simply "eMAT". In addition to functioning as a normal traction motor, the eMAT also functions as a power splitter, being capable of transmitting mechanical power while accompanying a continuously variable transmission (CVT) speed change from the vehicle moving-off mode (i.e., starting from a standstill). Based on the analysis and experiment, it is shown that the transmission efficiency of the eMAT is much higher than that of a conventional torque converter.

Another important consequence of developing the eMAT is to integrate multiple functions, such as EV driving, engine cranking, and CVT. As a result, unlike conventional parallel hybrid systems,[1,2] this system has the feature that a hybrid system can be constructed simply by replacing the conventional moving-off device with the eMAT in a conventional automatic transmission.

Moreover, the eMAT differs from a conventional power splitter[3] by transmitting power without a planetary mechanism. As a consequence, the eMAT further can function as a torsional damper, enabling it

to suppress engine vibration torque. In order to make use of this function in a powertrain system, this paper explores a control design concept for vibration suppression using the eMAT.

In previous research, a motor with the same structure has been studied. In Refs. (4)-(6), the electromagnetic field coupling of a compound motor structure is analyzed. Refs. (7) and (8) looked at the control problem of field decoupling between the two motors constituting the compound motor structure. The main focus of these studies was on the characteristics of each motor comprising the compound structure. Refs. (9) and (10) studied the CVT system characteristics. However, neither the transmission efficiency nor system losses in the drivetrain system using the compound motor structure has been clarified. Furthermore, few of these studies dealt with optimizing the system configuration.

Nevertheless, there are several challenges to applying the eMAT in a hybrid powertrain. One is the problem of brush wear in the slip ring system that enables us to supply electric power to the winding rotor. In our recent study,[11] we analyzed the wear characteristics of the brush, presented wear reduction measures, and thus improved the feasibility of using the slip ring system. Another problem is devising a structure that guarantees the cooling of the double rotor and the slip ring system. In our recent study, we also discussed solutions to these problems. Consequently, a prototype of the eMAT could be developed by combining these technologies, and all experiments discussed in this paper were conducted using the prototype built with these improvements.

2. eMAT and System Concept

2. 1 Electromagnetic Torque Converter

The structure of the eMAT is shown in **Fig. 1**. The eMAT is composed of an electromagnetic coupling (EMC), which can transmit torque between an input rotor and an output rotor, and a traction motor (TM), which can exchange electric and mechanical power between the stator and an output rotor. In this

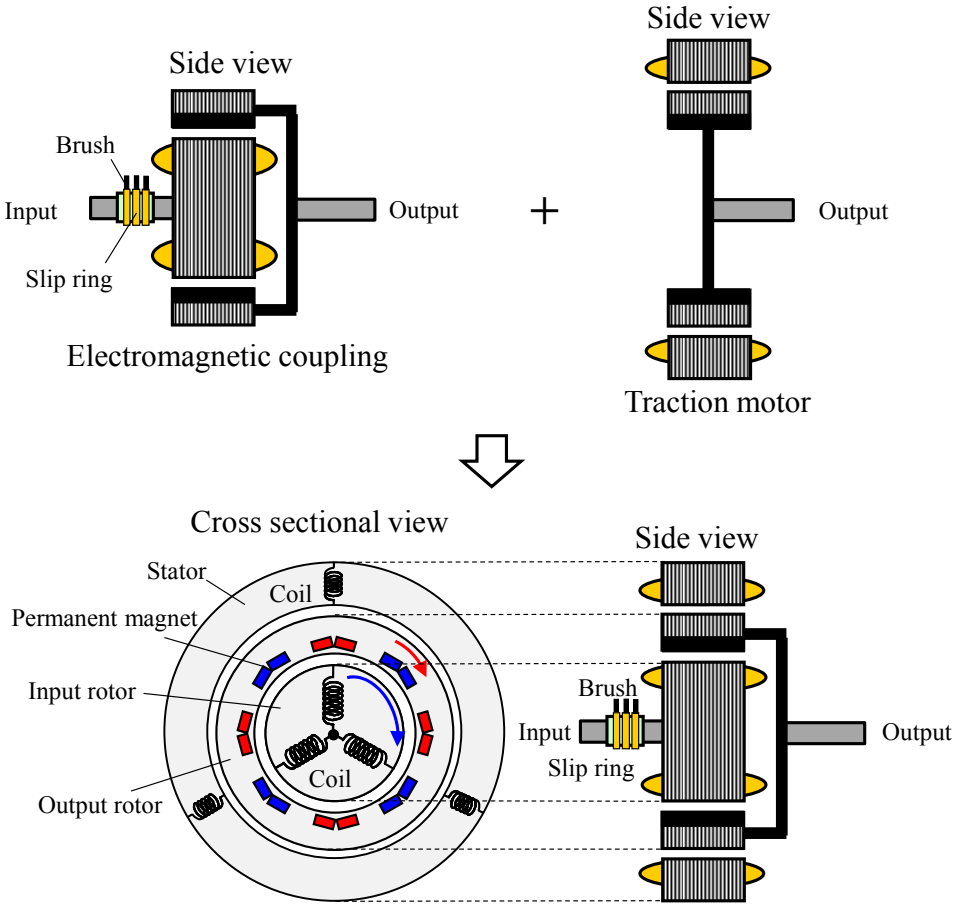

Fig. 1 Schematic of electromagnetic torque converter structure.

structure, by sharing the function of the output rotor between the EMC and the TM, one of the output rotors of the EMC or TM can be removed. A slip ring system, which is composed of a three-phase slip ring and brushes, is attached to the input rotor in order to supply current to the winding coils. By using the slip ring system, electric power is bi-directionally transferred between the EMC and an inverter.

Figure 2 shows the power flow for a fluid-type torque converter and the eMAT at a low gear ratio, where the input speed is higher than the output speed. In both converters, the input power is transferred by being split into two paths: a direct path where the input torque is directly transmitted and a derivative path where the power is generated in proportion to the relative speed of the input rotor and the output rotor. In a fluid-type torque converter, power is transferred by the medium of fluid oil without using controlling devices. In the eMAT, power is transferred by an electromagnetic force and electricity. Although the eMAT requires inverters, it enables us to control the transmitting torque, thereby regulating the input speed such that an internal combustion engine (ICE) is operated at its optimal condition. Furthermore, its drivability can be extended into the overdrive range, where the output speed is higher than the input speed. Additionally, due to the controllability of the inverters, the eMAT is capable of ICE cranking, EV driving, and regenerative braking.

2. 2 System Concept

Figure 3 shows the hybrid system configuration presented in this study. The system is composed of a conventional automatic transmission and the eMAT. The eMAT is an advanced substitute for a conventional fluid-type torque converter that is typically used with an automatic transmission. Compared with conventional moving-off devices, such as fluid-type torque converters and friction clutches, the eMAT has the following advantages:

(1) The eMAT has lower power loss than conventional moving-off devices. Hence, the transmission efficiency of the resultant hybrid system can be improved in comparison with hybrid systems in which the conventional devices are used.

(2) The eMAT can change the speed of the ICE continuously during ICE driving conditions, including vehicle moving-off. Consequently, this provides the benefits of a CVT, such as an improvement of system efficiency.

(3) The eMAT possesses multiple functions, i.e., ICE starting, electric motor driving, and regenerative braking.

(4) Additionally, the eMAT can transmit smooth torque to the output shaft even if the input torque is subject to fluctuations caused by the ICE.

Due to these advantages, by utilizing the eMAT with a mechanical transmission, a high-efficiency hybrid system can be constructed without appending a traction motor or an engine starter.

2. 3 Operating Modes

The eMAT hybrid system has three operating modes: power transmitting mode, ICE starting mode, and electric motor driving mode with regenerative braking.

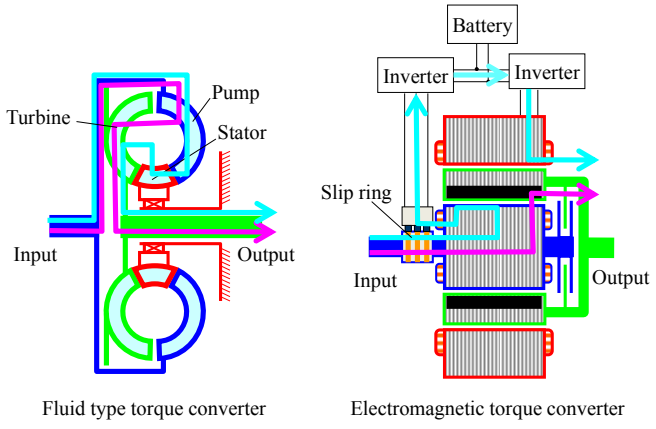

Fig. 2 Power flow for fluid-type torque converter and eMAT in moving-off mode.

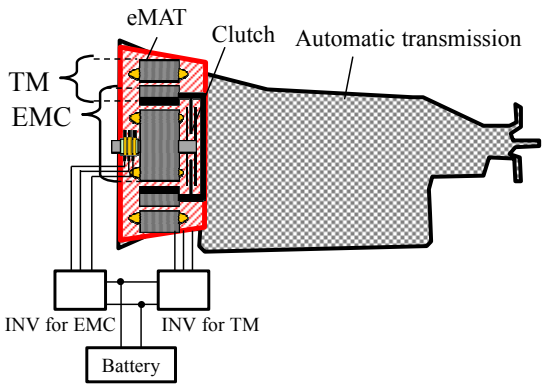

Fig. 3 Configuration of hybrid system with eMAT.

Power Transmitting Mode

In power transmitting mode, the ICE torque is transmitted to the output shaft by the EMC. When the input speed N_{in} is higher than the output speed N_{out}, motor torque generated by electric power from the EMC is added to the output shaft. Conversely, when the output speed is higher than the input speed, part of the transmitted engine torque on the output shaft is used to generate electric power to drive the EMC. The power flow is illustrated in **Fig. 4**.

Engine Starting Mode

In engine starting mode, the input rotor is driven by the output rotor while taking the reaction torque from the stator, thereby enabling engine cranking. This operation is available while the vehicle is stopped as well as in electric motor driving mode.

Electric Motor Driving and Regenerative Braking Mode

In electric motor driving mode, the traction motor drives the output rotor connected to a drive shaft. Since the input rotor is decoupled from the output rotor, this mode is available regardless of whether the engine is on or off.

3. eMAT Prototype

3. 1 Design Specifications

The eMAT prototype is based on the specifications shown in **Table 1**. These specifications are suitable for a hybrid truck with a 90-kW diesel ICE and an automatic transmission. **Table 2** shows the size and weight of the prototype, which has a compact structure that allows mounting on a vehicle. **Figure 5** is a cutaway view of the prototype design.

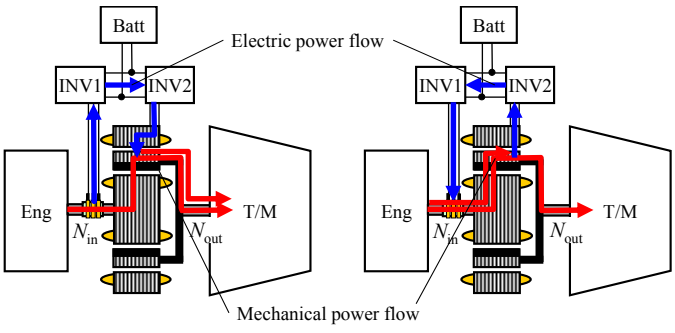

(a) $N_{in} > N_{out}$ Power split mode (b) $N_{in} > N_{out}$ Power circulating mode

Fig. 4 Power flow in power transmitting mode.

3. 2 Structure of the Prototype

Figure 6 provides more detail on the internal

Table 1 Design specifications of the eMAT.

Component	Max. Torque	Max. Speed	Max. Power
EMC	350 Nm	2500 rpm	35 kW
TM	350 Nm	4000 rpm	30 kW

Table 2 Size and weight of the prototype.

Size	Diameter, 450 mm Length, 286 mm
Weight	110 kg

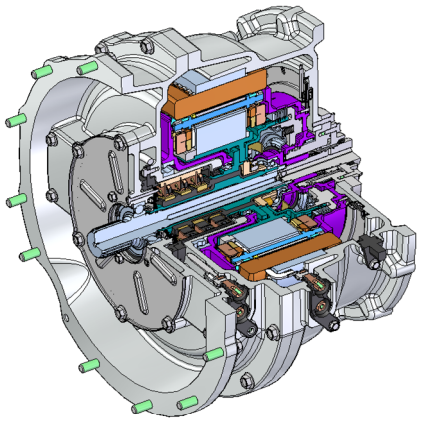

Fig. 5 Prototype of eMAT.

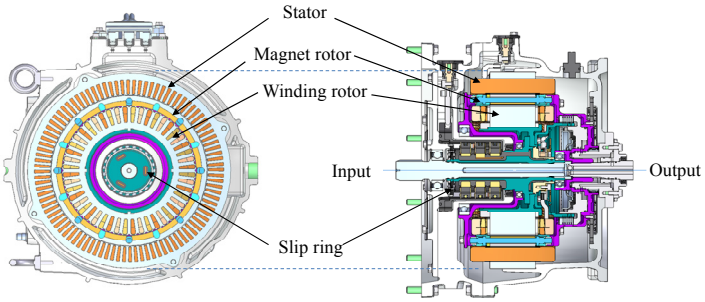

(a) Cross sectional view (b) Side view

Fig. 6 Internal structure of the eMAT prototype.

structure of the eMAT prototype. A set of two concentrically placed rotors is supported by bearings, and a stator is fixed to the casing. The set of rotors is arranged with a winding rotor inside a magnet rotor. The stator is placed outside the magnet rotor. A slip ring system is located inside the winding rotor (**Fig. 7**), which reduces the overall length of the eMAT. The slip ring system is indispensable for supplying power to the winding rotor and enabling the eMAT to generate coupling torque between the rotors. For other important design elements, such as cooling and brush wear suppression, refer to Refs. (11) and (14).

4. Transmission Efficiency

4. 1 Analysis

In principle, the eMAT is a CVT, so no other transmission gearing is required to change the speed ratio. However, the transmission efficiency of the eMAT deteriorates under overdrive conditions, where the speed ratio is well above 1. This can be confirmed by the following elementary formula for the transmission efficiency:

$$\eta = \begin{cases} \left\{ \dfrac{\eta_{\mathrm{emc}}\eta_{\mathrm{tm}}}{10^4} + \left(1 - \dfrac{\eta_{\mathrm{emc}}\eta_{\mathrm{tm}}}{10^4}\right) e \right\} \eta_{\mathrm{base}}, \; if \;\; e \le 1 \\ \left\{ \dfrac{10^4}{\eta_{\mathrm{emc}}\eta_{\mathrm{tm}}} - \left(\dfrac{10^4}{\eta_{\mathrm{emc}}\eta_{\mathrm{tm}}} - 1\right) e \right\} \eta_{\mathrm{base}}, \; if \;\; e > 1 \end{cases} . \quad (1)$$

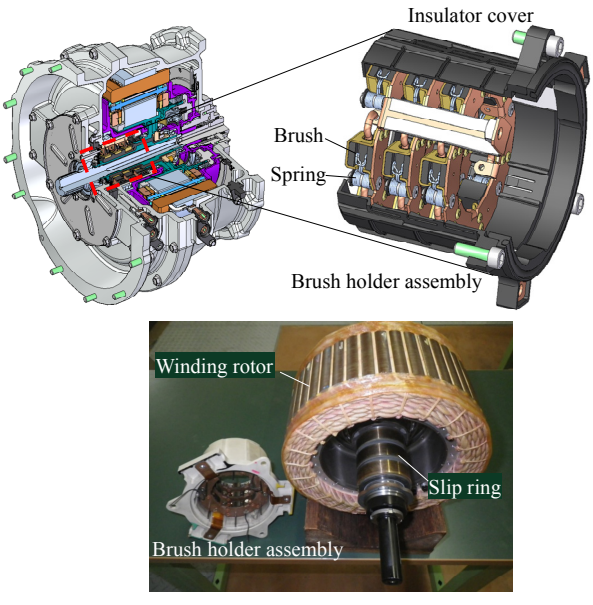

Fig. 7 Slip ring system designed for the eMAT.

where the speed ratio is defined by

$$e = \frac{N_{\mathrm{out}}}{N_{\mathrm{in}}} . \quad (2)$$

The efficiencies of the EMC and the TM are denoted by η_{emc} and η_{tm}, respectively, and the transmission efficiency for e = 1 is denoted by η_{base}. The transmission efficiency calculated using Eq. (1) is plotted in **Fig. 8**, where both η_{emc} and η_{tm} are assumed to be 90%. The change rate for the efficiency with respect to the speed ratio $|\partial\eta/\partial e|$ is plotted in **Fig. 9**, representing the deterioration rate of the transmission efficiency. It can be seen that the deterioration rate for $e > 1$ is larger than that for $e \le 1$.

Thus, in order to recover transmission efficiency in the overdrive range, the system configuration uses

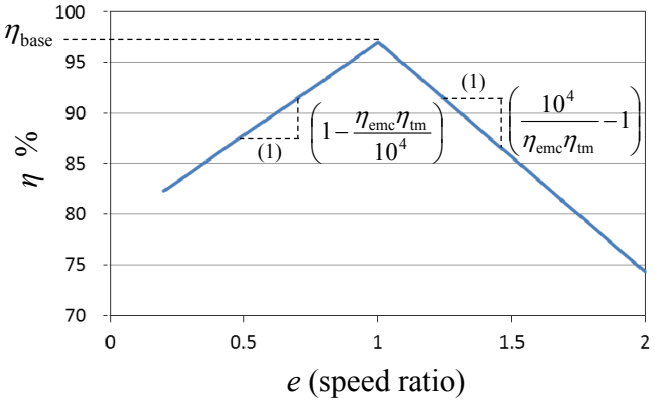

Fig. 8 Transmission efficiency for eMAT calculated using Eq. (1) under the assumption of $\eta_{\mathrm{emc}} = \eta_{\mathrm{tm}} = 90\%$.

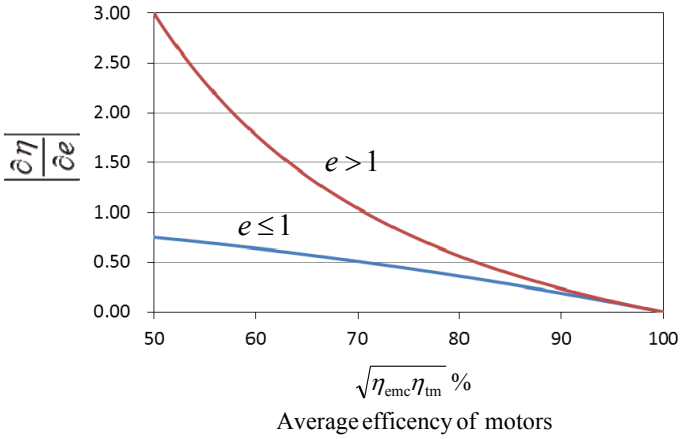

Fig. 9 Rate of change of transmission efficiency as function of average efficiency for $e \le 1$ and $e > 1$.

the mechanical transmission shown in Fig. 3. In this hybrid system, the efficiency can be maximized by using the mechanical transmission and a lock-up clutch that is installed between the rotors.

4. 2 Experimental Results

In order to measure the transmission efficiency, we constructed the motor bench system shown in **Fig. 10**. The eMAT prototype is attached to the motor bench system where both the input and output shafts are connected to a low-inertia dynamometer. The torques and rotational speeds of both the input and output shafts can be measured using the torque and speed meters installed on each shaft. The EMC and TM are controlled by each inverter, and the electric currents and voltages of the input and output ports of each inverter can be measured.

The transmission efficiency is defined as the ratio of the input power to the output power. Measurements are conducted under the condition that the battery power is zero. The transmission efficiency of the prototype is obtained from the measured data in the steady state as

$$\eta = \frac{T_{\text{out}} N_{\text{out}}}{T_{\text{in}} N_{\text{in}}} \times 100 \quad [\%], \tag{3}$$

where T_{in} and T_{out} denote the input and output torques, and N_{in} and N_{out} are the input and output rotational speeds, respectively. In **Fig. 11**, the transmission efficiency of the prototype is plotted, where e is the speed ratio defined by Eq. (2).

Figure 11 confirms that the maximum efficiency is attained when the speed ratio is nearly 1, and the efficiency deteriorates as the speed ratio decreases or increases from 1. This result is consistent with the analysis shown in Fig. 8, indicating that the system loss is minimized when the speed ratio is 1. Further, Fig. 11 compares the transmission efficiency for the eMAT and a fluid-type torque converter.[12] This comparison confirms that the eMAT improves the transmission efficiency at almost all speed ranges and allows the speed ratio to expand into the overdrive range, while keeping the efficiency flat when the speed ratio is nearly 1.

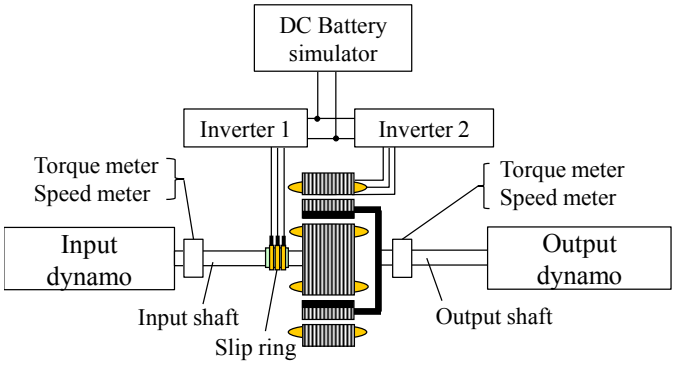

Fig. 10 Experimental motor test bench system.

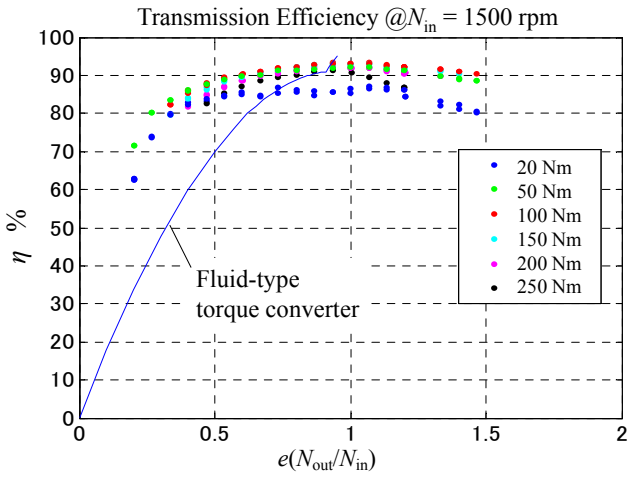

Fig. 11 Transmission efficiency of eMAT measured at input speed of 1500 rpm.

5. Vibration Torque Suppression

5. 1 Principle of Vibration Interception

The eMAT has a characteristic whereby the transmitted torque can be made arbitrarily smooth, even if the input torque includes vibration, as in the case of ICE torque. This is due to the contactless transmission structure, where the input shaft and the output shaft are mechanically decoupled. This is a unique feature not found in conventional power transmission devices. Hence, the eMAT is expected to be used as a unique power transmitting device by having a torsional damping function. In order to explore this characteristic, the two powertrain systems shown in **Fig. 12** are compared. In the eMAT powertrain, the output driveline is mechanically disconnected from the ICE, whereas in the traction motor powertrain, the output driveline is mechanically connected to the ICE.

Figure 13 compares the torque response of each system when vibration torque suppression is ideally performed. It can be seen that the output torque for each electric machine is different, while the vibration

torque is suppressed and a smooth torque is transmitted. The eMAT generates a smooth torque, whereas the traction motor generates a vibrating counter torque that cancels out the vibrating input torque. Generating the counter torque requires a precise prediction and the control of the vibrating torque that is to be transmitted to the input shaft of the traction motor. The eMAT does not require such estimation or control.

5. 2 Control Purpose

In order to utilize the eMAT as a CVT and further as a vibration suppression device, a design for control of the eMAT in a powertrain system is considered. In this case, the purposes of controlling the eMAT are:

(P1) Controlling the speed of the input rotor to track a reference speed such that the ICE can operate at its optimal thermal efficiency, and

(P2) Transmitting smooth torque to the output shaft, while suppressing the vibration torque generated by the ICE.

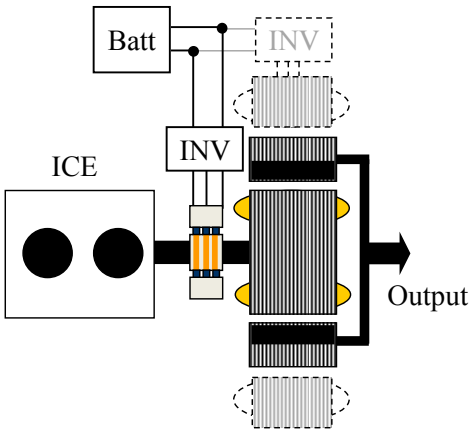

(a) eMAT

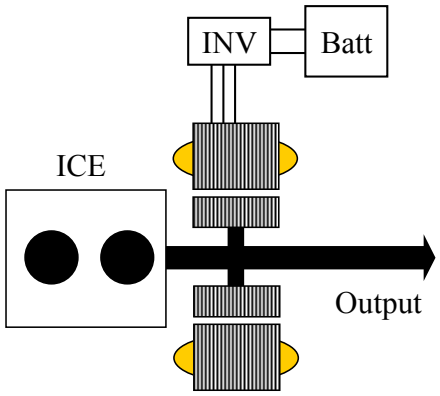

(b) Traction motor

Fig. 12 Comparison of powertrain architectures with (a) an eMAT and (b) a traction motor.

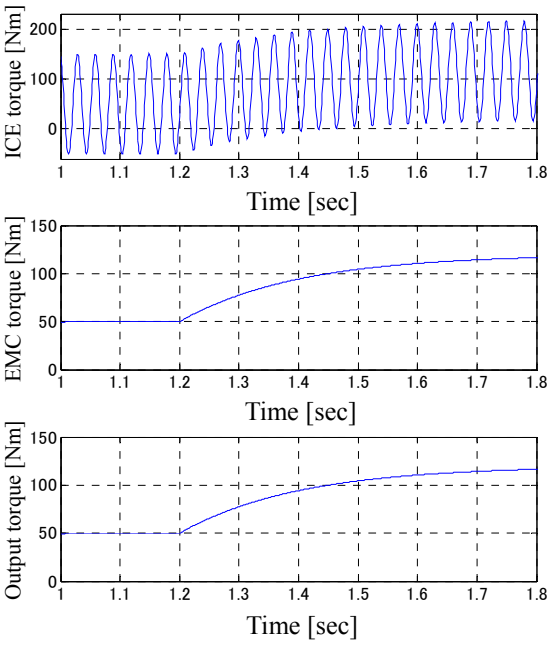

(a) eMAT

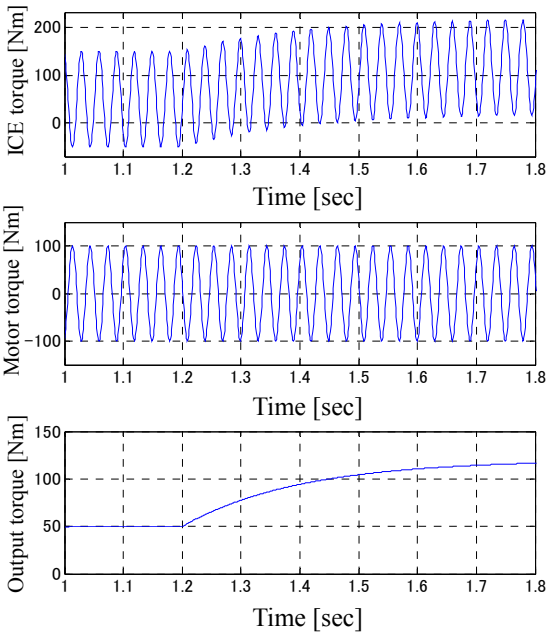

(b) Traction motor

Fig. 13 Comparison of vibration suppression for (a) an eMAT and (b) a traction motor.

5. 3 Mathematical Model

To achieve these purposes, a control system is designed based on a mathematical model representing the dynamical behavior of the input shaft of the eMAT. In the powertrain system with the eMAT, the input shaft comprises a crank shaft, flywheel, damper, slip ring, and winding rotor and can be represented by the two-inertia resonance model shown in **Fig. 14**.

For this model, the system equations can be written as

$$J_{\text{in}}\dot{\omega}_{\text{in}}(t) = T_{\text{in}}(t) - T_{\text{tor}}(t) - T_{\text{fin}}\,, \tag{4}$$

$$J_{\text{out}}\dot{\omega}_{\text{out}}(t) = T_{\text{tor}}(t) - T_{\text{EMC}}(t) - T_{\text{fout}}\,, \tag{5}$$

$$T_{\text{tor}}(t) = k\big(\theta_{\text{in}}(t) - \theta_{\text{out}}(t)\big) + c\big(\omega_{\text{in}}(t) - \omega_{\text{out}}(t)\big), \tag{6}$$

where t represents time, and other variables and physical parameters are defined in **Table 3**. For ease of analysis, the friction torques T_{fin} and T_{fout} are set to zero by including them in a viscous friction term in T_{tor}. By applying a Laplace transform to Eqs. (4) to (6) and setting the initial values of the variables to zero, we obtain the following equation:

$$\begin{pmatrix}\omega_{\text{in}}(s)\\ \omega_{\text{out}}(s)\end{pmatrix} = \begin{pmatrix}P_{11}(s) & P_{12}(s)\\ P_{21}(s) & P_{22}(s)\end{pmatrix}\begin{pmatrix}T_{\text{in}}(s)\\ -T_{\text{EMC}}(s)\end{pmatrix}, \tag{7}$$

where s is the Laplace transform variable and can take complex values. The transfer functions appearing in the above equation are represented as

$$\begin{pmatrix}P_{11}(s) & P_{12}(s)\\ P_{21}(s) & P_{22}(s)\end{pmatrix} = \frac{1}{poly(s)}\begin{pmatrix}J_{\text{out}}s^2 + cs + k & cs + k\\ cs + k & J_{\text{in}}s^2 + cs + k\end{pmatrix}, \tag{8}$$

$$poly(s) = s\left\{J_{\text{in}}J_{\text{out}}s^2 + \big(J_{\text{in}} + J_{\text{out}}\big)cs + \big(J_{\text{in}} + J_{\text{out}}\big)k\right\}. \tag{9}$$

A block diagram representing the input-to-output relationship of Eq. (7) is shown in **Fig. 15**.

Table 3 Notation

θ_{in} [rad]	Rotation angle of the input side
θ_{out} [rad]	Rotation angle of the output side
$\omega_{\text{in}} = \dot{\theta}_{\text{in}}$ [rad/s]	Angular speed of the input side
$\omega_{\text{out}} = \dot{\theta}_{\text{out}}$ [rad/s]	Angular speed of the output side
J_{in} [kg·m^2]	Moment of inertia of the input side
J_{out} [kg·m^2]	Moment of inertia of the output side
T_{in} [Nm]	Input torque to the input inertia
T_{tor} [Nm]	Torsional torque
T_{EMC} [Nm]	Output torque of EMC
c [Ns/rad]	Viscous damping coefficient
k [N/rad]	Spring constant
T_{fin} [Nm]	Friction torque of the input side
T_{fout} [Nm]	Friction torque of the output side

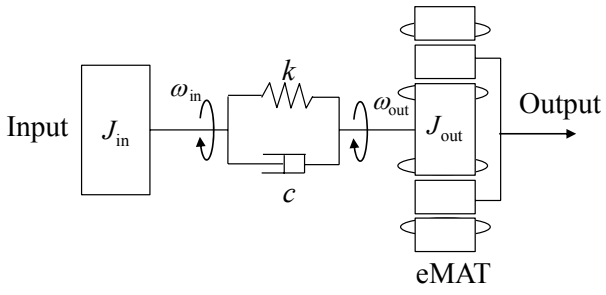

Fig. 14 Two-inertia resonance model representing the input shaft behavior of the eMAT powertrain system.

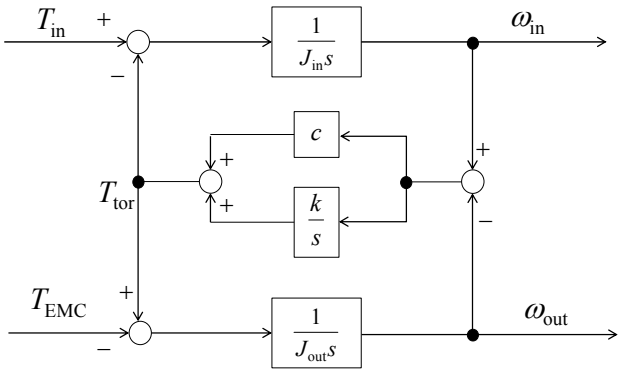

Fig. 15 Block diagram of the two-inertia resonance model of Fig. 14.

5. 4 Control Concept

In order to achieve control purpose (P1) described in Sec. 5.2, the feedback control system shown in **Fig. 16** is considered. A feedback controller $C(s)$ attempts to control the speed of the inner rotor to track the reference speed of the ICE under the input of a given ICE torque that consists of steady torque T_{st} and vibration torque T_{vib}. Strictly achieving this tracking performance allows the eMAT to transmit the given ICE torque as it is inputted. In this case, both the ICE vibration torque and steady torque are transmitted to the output of the driveline. Hence, in order to achieve both control purposes (P1) and (P2), a control concept of function separation by frequency band is introduced.

This control concept can be stated as follows. In the frequency band in which ICE vibration torque frequencies are present, feedback control is conducted such that the transmitting performance of the ICE torque to the output torque of the eMAT is insensitive. On the other hand, outside the frequency band of the ICE vibration torque, feedback control is conducted such that the speed tracking performance improves, thereby improving the transmitting performance of steady torque.

5. 5 Analysis of the Feedback Control System

The feedback control system that is based on the control concept is analyzed by introducing the following two transfer functions:

$$G_{\mathrm{T_{IO}}}(s) = \frac{P_{22}(s)C(s)}{1+P_{22}(s)C(s)} P_{22}{}^{-1}(s)P_{21}(s), \qquad (10)$$

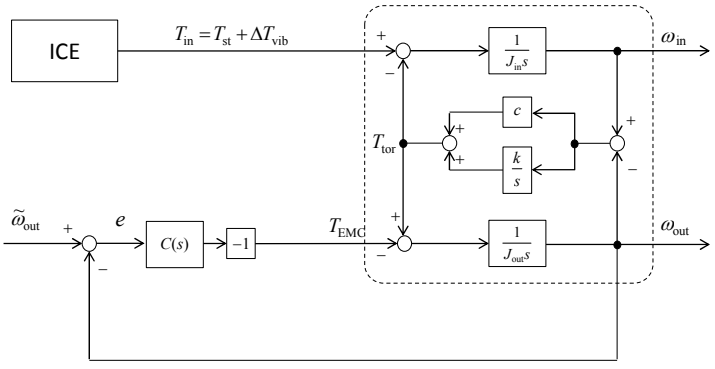

Fig. 16 Block diagram of the feedback control system for the two-inertia resonance system shown in Fig. 14.

$$S(s) = \frac{1}{1+P_{22}(s)C(s)}. \qquad (11)$$

The transfer function $G_{\mathrm{T_{IO}}}(s)$ represents the input-to-output relationship between the input torque T_{in} and the EMC output torque T_{EMC}, and function $S(s)$ represents the relationship between the reference speed $\tilde{\omega}_{\mathrm{out}}$ and the speed tracking error ε.

Assuming the frequency band of the ICE vibration torque to be $\Omega_{\mathrm{NV_{ICE}}}$, which represents a set of frequencies of the vibration torque, both control purposes (P1) and (P2) are attained by specifying

$$\left|G_{T_{IO}}(j\omega)\right| < \gamma_1, \quad \forall\omega \in \Omega_{\mathrm{NV_{ICE}}}, \qquad (12)$$

$$\left|S(j\omega)\right| < \gamma_2, \quad \forall\omega \in \overline{\Omega}_{\mathrm{NV_{ICE}}}, \qquad (13)$$

where $\overline{\Omega}_{\mathrm{NV_{ICE}}}$ represents the complementary set of $\Omega_{\mathrm{NV_{ICE}}}$, and γ_1 and γ_2 are design parameters that specify the relative weight of each constraint.

Vibration Torque Interception Structure

The transfer function $G_{\mathrm{T_{IO}}}(s)$ is composed of a control-dependent term

$$T(s) := \frac{P_{22}(s)C(s)}{1+P_{22}(s)C(s)}, \qquad (14)$$

which can be adjusted by the controller $C(s)$, and a structure-dependent term,

$$P_{22}{}^{-1}(s)P_{21}(s) = \frac{cs+k}{J_{\mathrm{in}}s^2+cs+k}, \qquad (15)$$

which is composed of only the physical parameters of the system and is independent of the control. Hence, the requirement given by the inequality (12) is achieved by the vibration suppression effect of the feedback control and a passive damping effect of a damping component of the powertrain system. This mechanism is shown schematically in **Fig. 17**. Thus, the powertrain system using the eMAT provides a new vibration suppression architecture, whereas conventional powertrain systems rely on only passive damping devices.

Function Separation by Frequency Band

Although requiring the controller to satisfy the inequality (12) improves the damping effect of the eMAT, the torque transmission performance is

decreased in the same frequency band. This can be explained by the following equation:

$$G_{T_{IO}}(s)\cdot P_{21}^{-1}(s)P_{22}(s)+S(s)=1. \quad (16)$$

Since the gain of $P_{21}^{-1}(s)P_{22}(s)$ is invariant regardless of the feedback controller $C(s)$, imposing the constraint given by the inequality (12) on $G_{T_{IO}}(s)$ makes the gain of $S(s)$ large in the same frequency band. Here, recall that fulfilling the ICE-speed tracking performance and the transmitting performance of the steady ICE torque requires the gain of $S(s)$ to be small. This implies that the performance of vibration torque suppression and ICE speed tracking cannot be improved simultaneously in the same frequency band. Hence, as specified in inequalities (12) and (13), these performance values are separated by an objective frequency band, as shown in **Fig. 18**.

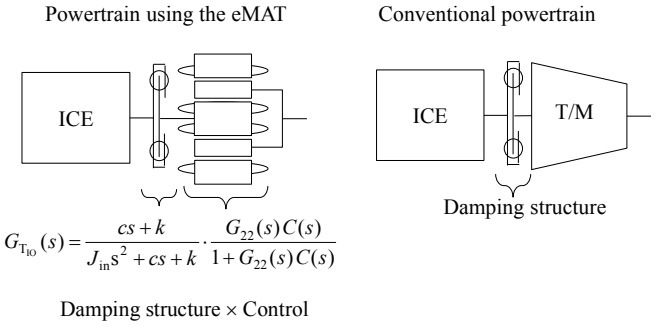

Fig. 17 Schematic diagrams of the damping structures of conventional and eMAT powertrain systems.

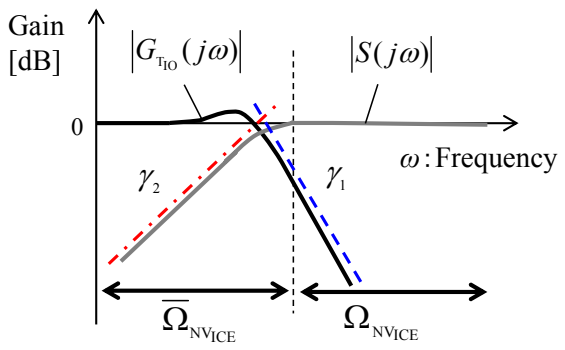

Fig. 18 Gain characteristics.

5. 6 Performance Improvement by Feedforward Control

In the previous section, the performances were shown to be separable by a frequency band. However, if the frequency band $\Omega_{NV_{ICE}}$ expands to a lower frequency, suppressing the vibration torque transmission reduces the performance of ICE speed regulation, thereby degrading the eMAT's torque response. This can occur when an ICE with few cylinders is used. This drawback is due to the fact that both vibration torque suppression and the torque response performance depend only on the feedback control.

The ICE torque in steady state can be estimated and used to directly generate the torque of the eMAT. In order to realize this, we introduced a feedforward control with

$$\hat{T}_{EMC}=FF(s)\hat{T}_{st}. \quad (17)$$

Figure 19 shows the structure of the control system. The variable $\hat{T}_{EMC}$ is the EMC torque generated by the feedforward control, and $\hat{T}_{st}$ is the estimated ICE torque in steady state. The feedforward controller $FF(s)$ is derived based on the system in Eq. (7) as

$$FF(s)=P_{22}^{-1}(s)P_{21}(s)=\frac{cs+k}{J_{in}s^2+cs+k}. \quad (18)$$

6. Demonstration Experiment

To confirm the effects of the proposed control concept, we tested it using the motor bench system shown in Fig. 10. Details of the control system

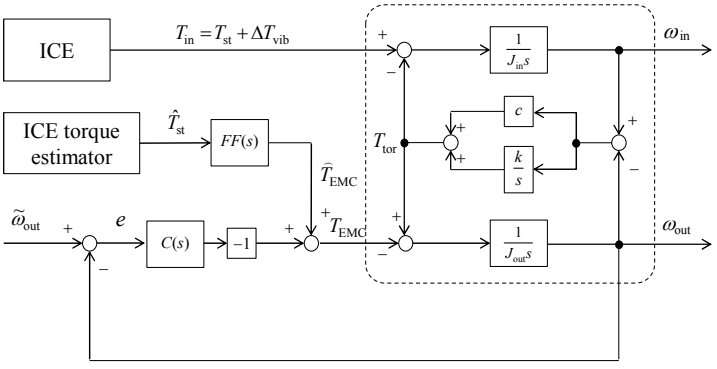

Fig. 19 Feedforward control system structure of the EMC.

design are given in Ref. (15). From a priori information, it is known that this system has a resonance frequency of 23.5 Hz. This is due to a torsional resonance of the input shaft of the eMAT. An input dynamo generated steady-state input torque with a vibration. Additionally, to confirm the tracking performance for torque and speed, the input torque in steady state was changed stepwise.

Figure 20 shows the input torque and the transmitted torque, and **Fig. 21** shows both the input-side and output-side inertia speeds of the input shaft. Frequency spectra of both torque signals are plotted in **Fig. 22**. From these figures, it is seen that the EMC transmits a steady torque without causing torsional vibration, while suppressing the vibration torque of 33.3 Hz and

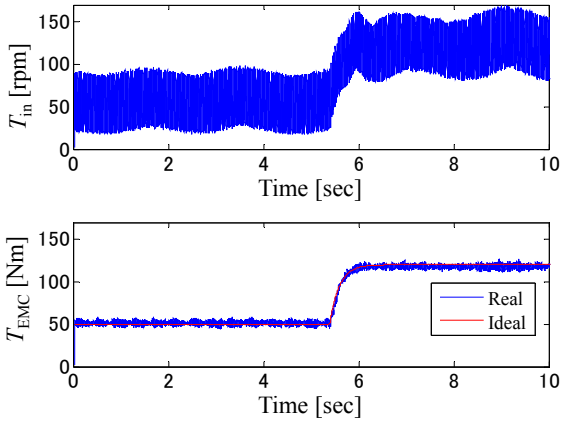

Fig. 20 Input torque (T_{in}), comprising both steady and vibration torque (33.3 Hz), versus transmitted EMC torque (T_{EMC}), showing the damping effect and improved tracking performance.

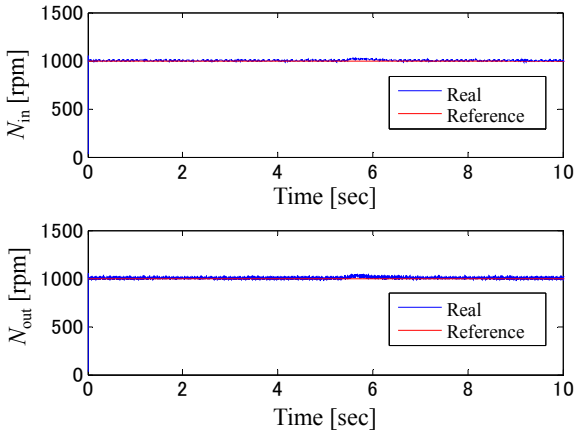

Fig. 21 Tracking performance of the input speed as the input torque changed. Both speeds of input shaft track the reference, avoiding torsional resonance in the input shaft.

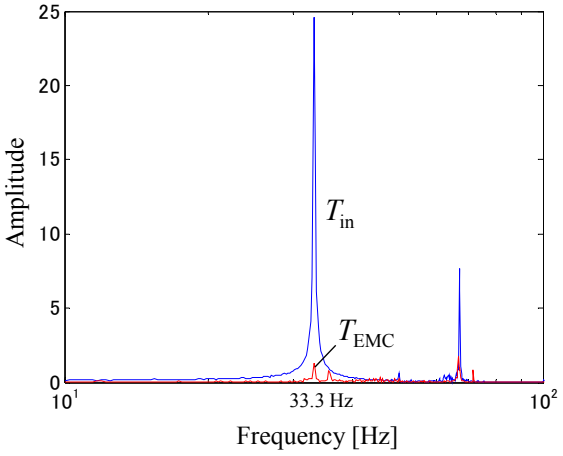

Fig. 22 Frequency spectra of the input torque and transmitted torque.

maintaining the tracking performance of the input speed and the transmitting torque to their respective references as the input torque changed.

7. Conclusion

This paper presented a new electric machine, the eMAT, and proposed a hybrid system configuration aimed at improving fuel economy. Integrating useful, multiple functions into an all-in-one mechanism, the eMAT can be utilized to construct a compact high-efficiency hybrid system. To validate the eMAT, a prototype was developed and tested in a motor bench system. The result showed that the transmission efficiency in the vehicle moving-off mode can be improved in comparison with a conventional torque converter. The eMAT can be the most efficient moving-off device that also integrates the functions of a CVT and electric motor driving. Further, this paper clarified a new inherent function of vibration suppression, which arises from the eMAT structure. Then, in order to make full use of the new function with the other functions as a CVT, we presented a control design using the eMAT.

References

(1) Hayasaki, K., Abe, T., Tanishima, K., and Chujo, K., "Development of a Parallel Hybrid System for RWD Vehicles", *SAE Int. J. Engines,* Vol. 4, No. 1 (2011), pp. 1071-1087.

(2) Gitt, C., Maisch, M., and Kiesel, J., "New Mercedes-Benz Hybrid Transmission with Increased Power Density", *12th Int. CTI Symp., Automot. Transm., HEV and EV Drives* (2013).

(3) Muta, K., Yamazaki, M., and Tokieda, J., "Development of New-generation Hybrid System THS II - Drastic Improvement of Power Performance and Fuel Economy", *SAE Tech. Pap. Ser.,* No. 2004-01-0064 (2004).

(4) Nordlund, E., and Sadarangani, C., "The Four-Quadrant Energy Transducer," *Proc. IEEE Ind. Appl. Soc. Meet.,* No. 10 (2002), pp. 13-18.

(5) Eriksson, S., and Sadarangani, C., "A Four-Quadrant HEV Drive System", *Proc. IEEE Vehicular Tech. Conf.* (2002), pp. 1510-1514.

(6) Tao, F., Xuhui, W., Jingwei, C., and Xizheng, G., "Permanent Magnet Dual Mechanical Port Machine Design for Hybrid Electric Vehicle Application", *Proc. IEEE Int. Conf. Ind. Technol.* (2008), pp. 1-5.

(7) Xuhui, W., Feng, Z., Xinhua, G., Tao, F., Longya, X., and Qiongxuan, G., "Application of PM Type DMPM in Hybrid Electric Vehicle", *Proc. Energy Convers. Congr. and Expos.* (2010), pp. 1144-1149.

(8) Liu, Y., Tong, C., Liu, R., Zhao, J., Bai, J., and Zheng, P., "Comprehensive Research on Compound-structure Permanent-magnet Synchronous Machine System Used for HEVs", *Proc. IEEE Energy Convers. Congr. and Expos.,* No. 2 (2010), pp. 1617-1622.

(9) Xinhua, G., Xuhui, W., Jingwei C., Feng, Z., and Xizheng, G., "Simulation of an Electrical Variable Transmission Based on Dual Mechanical Ports Electric Machine with Clutch", *Proc. IEEE Vehicle Power and Propul. Conf.* (2008), pp. 1-5.

(10) Hoeijmakers, M. J., and Rondel, M., "The Electrical Variable Transmission in a City Bus", *Proc. IEEE Power Electr. Spec. Conf.* (2004), pp. 2773-2778.

(11) Asami, S., Watanabe, T., Tominaga, S., and Murakami, A., "New Slip Ring System for Electromagnetic Coupling in HEV Driveline", *SAE Tech. Pap. Ser.,* No. 2016-01-1222 (2016).

(12) Ota, H., Nozaki, K., Honda, A., Kinoshita, M. et al., "Toyota's World First 8-speed Automatic Transmission for Passenger Cars", *SAE Tech. Pap. Ser.,* No. 2007-01-1101 (2007).

(13) Zhou, K., Glover, K., and Doyle, J. C., *Robust and Optimal Control* (1996), 596p., Prentice Hall.

(14) Watanabe, T., Tsuchiya, E., Ebina, M., Osada, Y., Toyama, T., and Murakami A., "High Efficiency Electromagnetic Torque Converter for Hybrid Electric Vehicles", *SAE Int. J. Alt. Power,* Vol. 5, No. 2 (2016), pp. 228-236.

(15) Watanabe, T., Fujiyoshi, T., and Murakami, A., "Vibration Torque Interception Using Multi-functional Electromagnetic Coupling in a HEV Drive Line", *SAE Int. J. Alt. Power,* Vol. 5, No. 1 (2016), pp. 157-166.

Takao Watanabe

Research Fields:
- System Control Engineering
- Electric Machines and Advanced Powertrain
- Control of Fuel Cell Vehicles

Academic Degree: Dr.Eng.
Academic Societies:
- The Society of Instrument and Control Engineers
- Society of Automotive Engineers of Japan

Shu Asami

Research Fields:
- Experiment and Analysis of Slip Ring System
- Development of Auto Parking System

Eiji Tsuchiya

Research Fields:
- Mechanical Engineering
- Transmission
- Hybrid Vehicle System

Masaki Ebina

Research Field:
- Power Train System and Control

Academic Societies:
- Society of Automotive Engineers of Japan
- The Japan Society of Mechanical Engineers

Yasumitsu Osada

Research Field:
- Mechatronics System Design

Tomoyuki Toyama*

Research Field:
- Drivetrain System Development of Vehicle

Academic Society:
- Society of Automotive Engineers of Japan

Akira Murakami**

Research Field:
- Advanced Drivetrain Engineering

Academic Society:
- Society of Automotive Engineers of Japan

* Aisin Seiki Co., Ltd.
**Toyota Motor Corporation

